Cleanliness Evaluation of Rough Surfaces with Diffuse IR Reflectance

L. H. Pearson
Thiokol Corporation
P.O. Box 707, M/S 244
Brigham City, Utah 84302

Abstract

Contamination on bonding surfaces has been determined to be a primary cause for degraded bond strength in certain solid rocket motor bondlines. Hydrocarbon and silicone based organic contaminants that are airborne or directly introduced to a surface are a significant source of contamination. Diffuse infrared (IR) reflectance has historically been used as an effective technique for detection of organic contaminants, however, common laboratory methods involving the use of a Fourier transform IR spectrometer (FTIR) are impractical for inspecting the large bonding surface areas found on solid rocket motors. Optical methods involving the use of acousto-optic tunable filters and fixed bandpass optical filters are recommended for increased data acquisition speed. Testing and signal analysis methods are presented which provide for simultaneous measurement of contamination concentration and roughness level on rough metal surfaces contaminated with hydrocarbons.

Introduction

IR reflection spectroscopy is an analytical methodology that has been applied previously to the problem of surface and thin film characterization (1-3). More specifically, diffuse reflectance IR spectroscopy has been evaluated for detection of organic contaminants on bonding surfaces (4-6) and has been found to be effective for detection of contaminants with sufficiently strong IR absorption bands. The use of IR spectroscopy allows both the detection and identification of contaminant types since each has a characteristic absorption spectrum (fingerprint). However, the use of laboratory analytical FTIR instrumentation is not practical for on-line inspection or mapping of large bonding surface areas such as those found on solid rocket motor components the size of the Shuttle and large strategic defense motors. In addition to the rapid data acquisition requirements imposed by their large size, surfaces on solid rocket motors tend to be rough, such as grit blasted metal surfaces, or machined surfaces of fiber filled polymeric materials. Roughness has a tendency to lower signal to noise ratios and thus may impose additional constraints on optical design.

Contaminants most commonly found on solid rocket motor bonding surfaces are either hydrocarbon or silicone based and are introduced by direct contact with tooling or personnel, or environmentally introduced via airborne particulates that are deposited on the surface. When these contaminants are found on rough metal surfaces, diffuse IR reflectance methods must be able to find the contaminant in the presence of roughness and further, must be able to distinguish contaminant concentration variations from roughness variations. Optical methods and data acquisition and reduction methods for providing speed and reliable detection of hydrocarbon contamination on rough (grit blasted) metal surfaces are specifically addressed in this paper.

Methodology

Hydrocarbons can be readily detected on a surface by looking for the presence of their characteristic carbon-hydrogen (C-H) stretch band at about 3.4 micrometers (μm). Previous work (4) has indicated that backscattered IR methods provide greater sensitivity to small concentrations of contaminants on rough metal surfaces than do specular methods. Backscatter optics must be coupled with a means for rapid detection of scattered light intensity over a continuous band of wavelengths or at several discrete narrow wavelength bands that include the 3.4 μm absorption band and at least two reference wavelength bands (side-bands). This is accomplished by using an acousto-optic tunable filter (AOTF) for continuous or discrete wavelength band detection, or by using fixed band-pass filters for discrete wavelength band detection. Figures 1 and 2 show schematic diagrams for these two optical methods. Both the AOTF and the discrete optical filter methods shown in the figures provide sufficiently rapid data acquisition capability so that an instrument based on either method can collect data on-the-fly when scanned over a surface at speeds up to a few inches per second. Hence, measurement rates on the order of 10's to 100's of complete spectral measurements (described below) per second are achievable. The AOTF optical method is described in detail in reference (4) and will not be further described in this paper. The discrete optical filter method, shown in Figure 2, splits the scattered beam into three beams by using spectral beam splitters and band-pass filters. Each beam has its own detector, hence, parallel data collection is made possible for each wavelength band, significantly increasing data collection speed. A more complete description of this optical setup is found in reference (7). All data presented in this paper was obtained with the discrete optical filter design implemented in a packaged instrument cooperatively developed by TMA Technologies and Thiokol Corporation and given the trade name of SurfMap-II™.

The objective of the optics is to rapidly obtain measurements from which the peak height of the C-H stretch absorption band is determined. The required measurements are the absorbance at two side-band wavelengths, with one on each side of the band peak, and the absorbance at the wavelength of the band peak. Figure 3 shows the spectrum of the C-H stretch absorption band for a typical hydrocarbon contaminant with the wavelength bands of the three measurements indicated. In order to determine the peak absorbance, a line is fit to the two side-band measurements to approximate the baseline of the spectrum. The interpolated value of the baseline at the wavelength of the peak is subtracted from the measured peak absorbance. The resultant value, ΔA, is indicated in Figure 3 and has been found to be directly related to contamination concentration (4-6). The process is mathematically described below.

The linear approximation of the absorption spectrum baseline is calculated from

1) $A_b(\lambda) = a + b\,\lambda$

where a and b are constants determined from the side-band measurements, 1 and 2, shown in Figure 3, and λ is the wavelength. Constants a and b are given by

2) $b = (A_2 - A_1) / (3.7\text{-}3.2) = (A_2 - A_1) / 0.5$

3) $a = A_1 - b\,(3.2)$

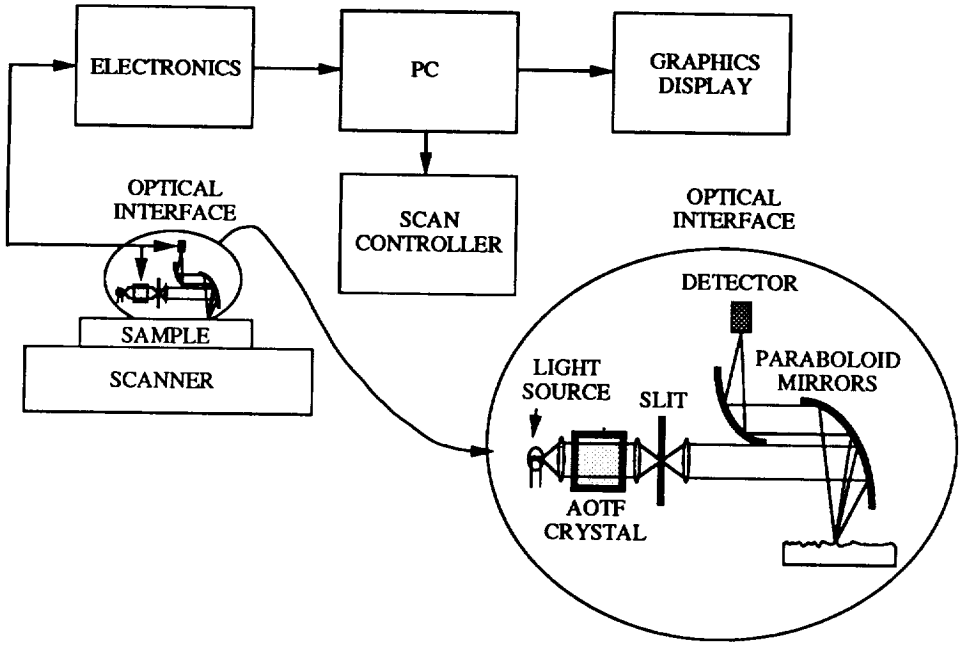

Figure 1. Schematic diagram for AOTF based optical setup.

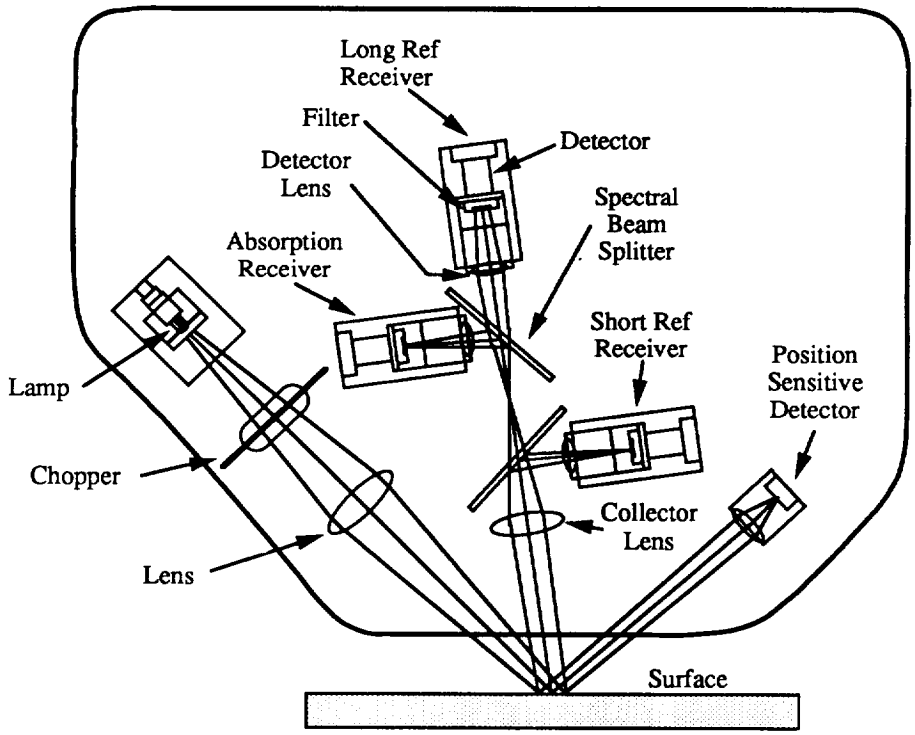

Figure 2. Schematic diagram for discrete band-pass filter based optical setup.

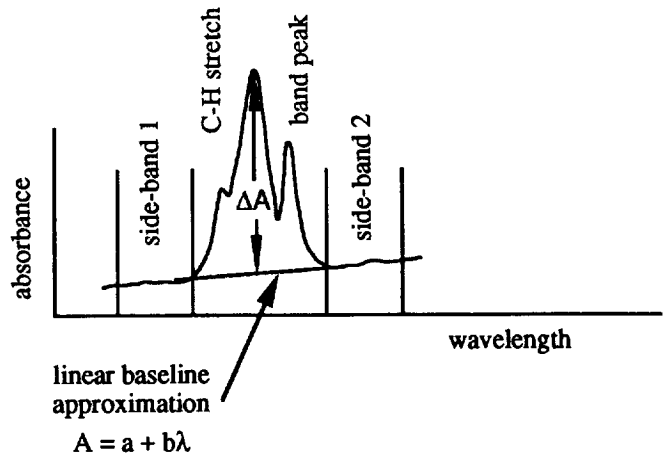

Figure 3. Typical C-H stretch absorption band with filter band locations indicated.

---

where A_1 and A_2 are the measured absorbances for the two side-band wavelengths. For the C-H stretch absorption band, side-band 1 wavelength is assumed to be 3.2 μm, side-band 2 wavelength is assumed to be 3.7 μm, and the peak wavelength is assumed to be 3.4 μm for the specific optical filters used in the SurfMap-II™. Using equation 1, ΔA is calculated from

4) $$\Delta A = A_p - A_b(\lambda=3.4)$$

where A_p is the measured absorbance at the C-H stretch band peak.

The absorbance measurements A_p, A_1, and A_2 are determined from the backscattered IR light power measured from the surface and from corresponding measurements taken from a clean reference plate with a known average root mean square roughness (RA). That is,

5) $$A_1 = - \log_{10}(P_{1s}/P_{1ref})$$

6) $$A_2 = - \log_{10}(P_{2s}/P_{2ref})$$

7) $$A_p = - \log_{10}(P_{ps}/P_{pref})$$

The quantities P_{1s}, P_{2s}, and P_{ps} are the measured backscattered power levels from the sample surface at the respective wavelengths, 3.2, 3.7, and 3.4 μm. Likewise, P_{1ref}, P_{2ref}, and P_{pref} are the corresponding power measurements for the clean reference plate.

Subtracting the baseline from the peak absorbance measurement is important as it has been determined experimentally that this procedure significantly reduces the effect of roughness variations on the measurement as will be further discussed in the next section. The SurfMap-II™ performs the calculations listed above and outputs a, b, and ΔA in the form of a computer image file which is constructed while raster scanning the instrument over a surface.

Since The effect of roughness on absorbance measurements is reduced by applying

equation 4, it is plausible that one or both of the constants a and b in equation 1 relate to roughness. In the following section, it is shown that the baseline slope, b, can be correlated with RA.

Results

A series of grit blasted steel (D6AC) plates with clean surfaces and known RA roughness were mapped with the SurfMap-II™. The average ΔA, a, and b were determined from scan data for each plate. Reference measurements were taken from a clean plate with known RA. These tests were repeated several times using reference plates with different RA values. The average ΔA, a, and b values were plotted with respect to average RA for each plate and it was found that b was proportional to the difference between the RA of the sample and the RA of the reference plate. That is,

8) $$RA - RA_{ref} = S_b\, b$$

where S_b is a proportionality constant determined by linear regression.

The samples were then prepared with known concentrations (approximately 5, 10, and 15 mg/ft^2) of a hydrocarbon grease (CONOCO HD-2). Measurements of average ΔA, a, and b were repeated and it was further found that b was insensitive to the presence of contamination at these low concentrations. Hence, b provides an independent measurement of surface RA if RA_{ref} is known and S_b has been determined. Figure 4 shows a plot of RA-RA_{ref} verses b for all measurements from both clean and contaminated samples.

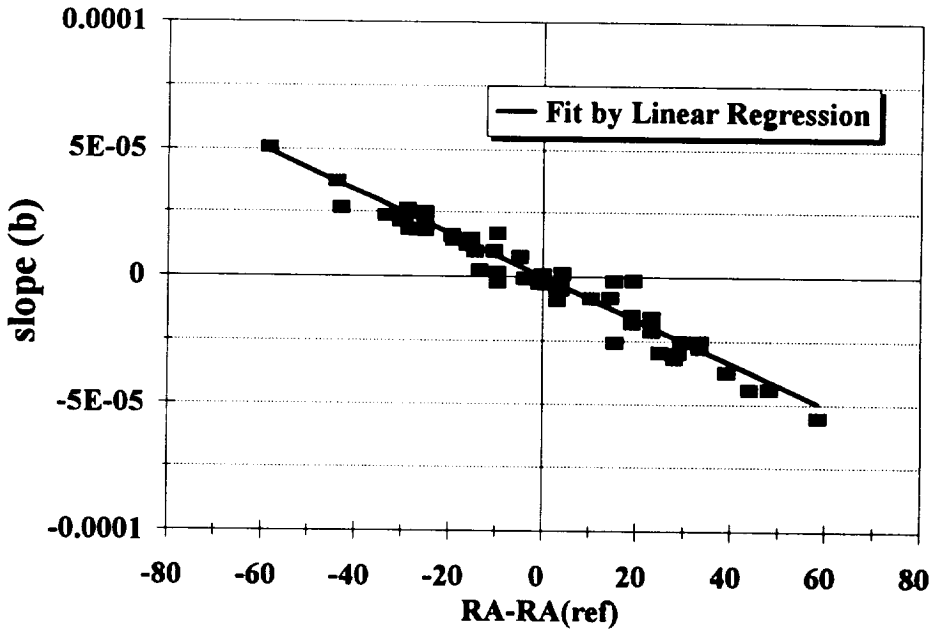

Figure 4. Dependence of approximated spectrum baseline slope, b, on RA.

When correlating ΔA with RA and with contamination concentrations it was found that ΔA is strongly dependent upon contamination concentration as expected since ΔA is a measure of the C-H band peak height, but it is also weakly dependent on roughness, that is, upon RA-RA_{ref}. The dependence on RA-RA_{ref} was found to be linear, but the slope of the line was empirically determined to be quadratically related to contamination concentration (see Figure 5) and the intercept was found to be proportional to contamination concentration (see Figure 6). That is,

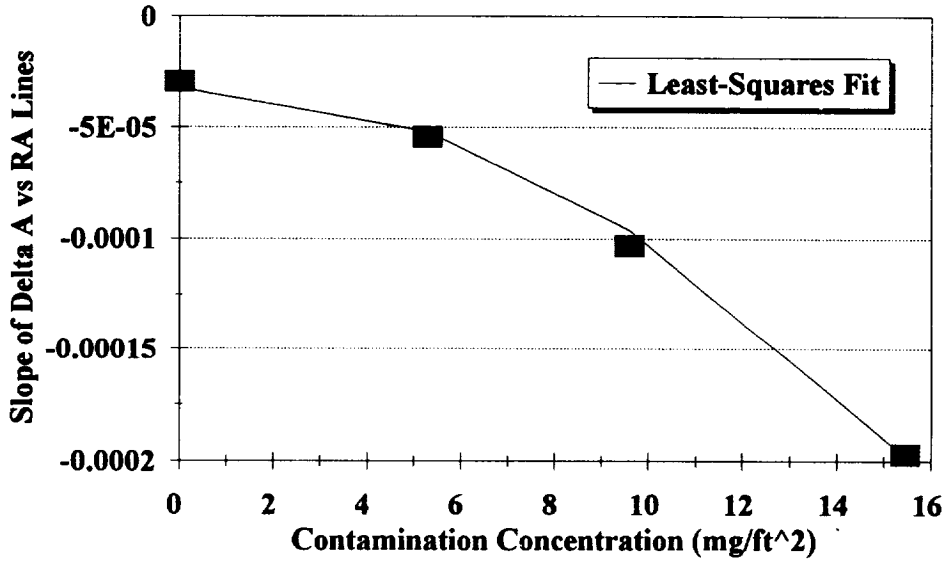

Figure 5. Dependence of slope ($S_{\Delta A}$) of ΔA verses RA curves on contamination concentration.

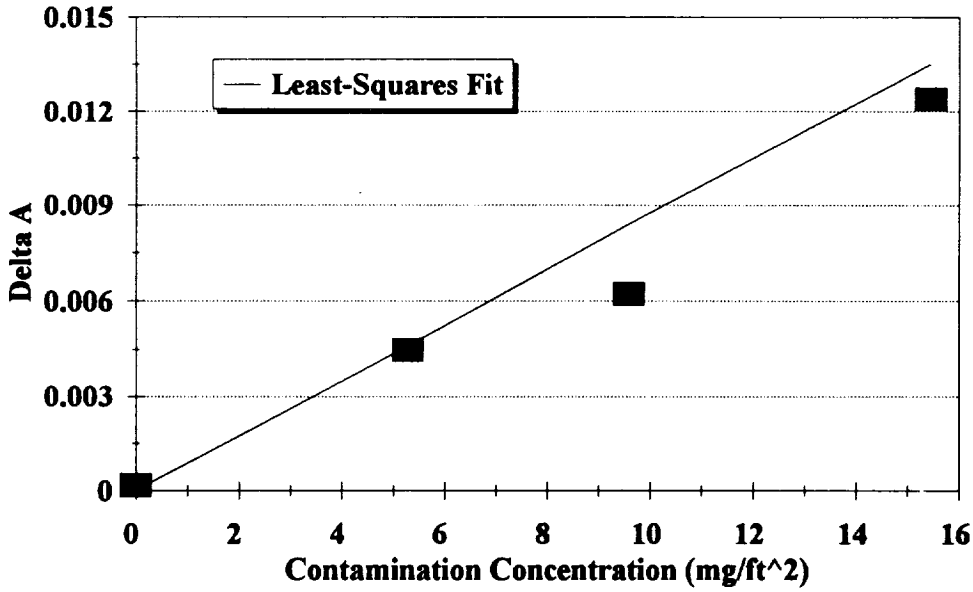

Figure 6. Dependence of ΔA on contamination concentration.

9) $\Delta A = \Delta A_{ref} + S_{\Delta A} (RA - RA_{ref})$

where

10) $\Delta A_{ref} = S_c h$

11) $S_{\Delta A} = y_s + S_s h^2$

Substituting equations 10 and 11 into equation 9 gives

12) $\Delta A = S_c h + [y_s + S_s h^2] S_b b$

The known hydrocarbon contamination concentration is h, and S_c, y_s, and S_s are constants determined by a least-squares fit of measured ΔA, b, and known h to equation 12.

When $RA = RA_{ref}$, it is found that $b = 0$ and equation 12 becomes

13) $\Delta A = S_c h$

It is observed that the second term in equation 12 is the correction for RA when RA_{ref} is different than RA for the sample (when $b \neq 0$). When the constants, S_c, y_s, S_s, and S_b have been determined, it is possible to estimate the roughness corrected contamination concentration from

14) $$h = \frac{-S_c + [S_c^2 - 2 S_s S_b b (y_s S_b b - \Delta A)]^{1/2}}{2 S_s S_b b}$$

which is obtained by solving equation 12 for h. If roughness is ignored, then contamination concentration is estimated from equation 10 by solving for h to give

15) $h = \Delta A / S_c$

Figure 7 shows the correlation of estimated h with known h when using equation 15 and Figure 8 shows the correlation using equation 14. Note that when correcting for RA (using equation 14), the data spread is reduced measurably so that at low contamination concentrations (h near zero), the accuracy is improved by about a factor of 2 from about $\pm$ 2 mg/ft^2 to about $\pm$1 mg/ft^2.

Conclusions

Optical methods have been recommended for providing rapid acquisition of absorbance data needed for detecting hydrocarbon contaminants on rough metal bonding surfaces. Signal processing methods have been developed for allowing simultaneous determination of contamination concentration and RA roughness. These optical and signal analysis tools provide a practical system for on-line inspection of large area bonding surfaces such as is found on solid rocket motors.

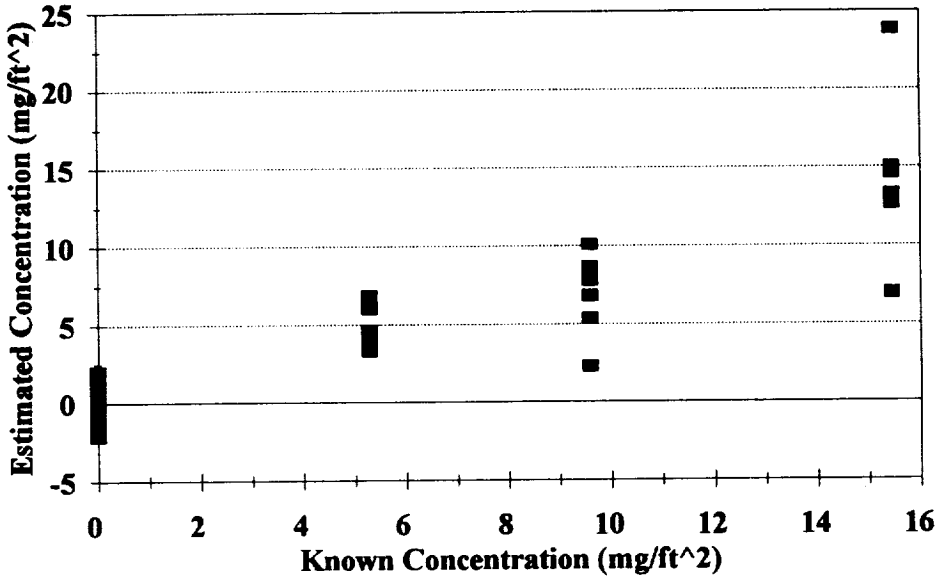

Figure 7. Contamination concentration estimate from ΔA measurement compared with known concentration without correction for RA (equation 15).

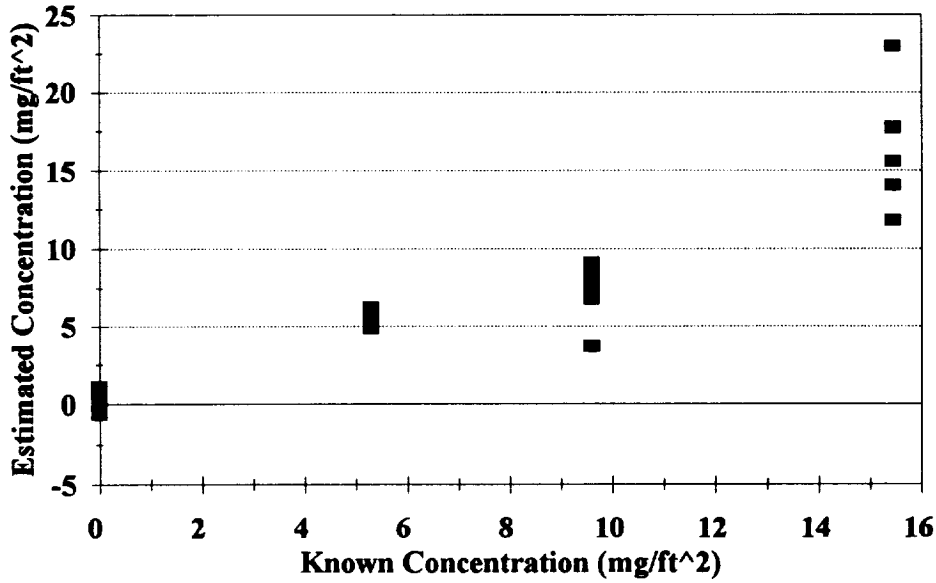

Figure 8. Contamination concentration estimate from ΔA measurements compared with known concentration using RA corrected equation 14.

References

1. Hansen, W. N., "Reflection Spectroscopy of Adsorbed Layers," Symposium of the Faraday Society, 1970, No. 4, pp. 27-35.

2. Hansen, W. N., "Reflection Spectroscopy of Optical Coatings," J. Opt. Soc. Am., Vol. 69, No. 2, 1979, pp. 264-272.

3. Hansen, W. N., Pearson, L. H., and Hansen, G., "Characterization of Small Absorptions in Optical Coatings," Laser Induced Damage in Optical Materials, NBS Spec. Publ. 568, 1979, pp. 247-251.

4. Pearson, L. H., "Bond Surface Contamination Imaging Using an AOTF Spectrometer," Review of Progress in Quantitative Nondestructive Evaluation, Vol. 12, Edited by D. O. Thompson and D. E. Chimenti, Plenum Press, New York, 1993, pp. 1619-1623.

5. Pearson, L. H., "Diffuse Reflectance IR Spectroscopy for Bonding Surface Contamination Characterization," Review of Progress in Quantitative Nondestructive Evaluation, Vol. 10, Edited by D. O. Thompson and D. E. Chimenti, Plenum Press, New York, 1991, pp. 581-588.

6. Pearson, L. H., "IR Spectroscopy for Bonding Surface Contamination Characterization," Review of Progress in Quantitative Nondestructive Evaluation, Vol. 9, Edited by D. O. Thompson and D. E. Chimenti, Plenum Press, New York, 1990, pp. 2017-2024.

7. Swimley, B. D., Knighton, M. W., Khurdal, V. C., Pearson, L. H., Stover, J. C., "Design review of an Instrument to Map Low-Level Hydrocarbon Contamination," Proc. SPIE, 1995-10, July 1993, pp 92-100.